J. Fluid Mech. (1986), *vol.* 168, *pp.* 383–392
Printed in Great Britain

Starting flow over spoilers, double steps and cavities

By F. FINAISH, P. FREYMUTH AND W. BANK
Department of Aerospace Engineering Sciences, University of Colorado, Boulder, Colorado 80309, USA

(Received 14 October 1985)

The development of two-dimensional vortex patterns in accelerating flow starting from rest has been investigated by streakline visualization and documented in photographic sequences. We considered flow over spoilers, double steps and cavities. A limited parametric analysis is provided for some of the photographic results.

1. Introduction

The development of vortex patterns in dynamically separating flows is very complex and considerable skill is needed for its description. A recent review of this research area by Freymuth (1985) provided a descriptive vocabulary with application to accelerating flow around airfoils. The purpose of this paper is to consider additional flow geometries and to extend the description of vortex pattern developments to these new areas. We concentrated on accelerating flow over spoilers, steps and cavities because their geometries differ considerably from those of airfoils. Emphasis is on new pattern developments with only minor parametric exploration.

The scientific literature does not contain any references to acelerating flow over spoilers, double steps or cavities; however other types of flow for these geometries can be referred to.

Steady flow over an oscillating spoiler has been investigated by Francis *et al.* (1979). Koga, Reisenthel & Nagib (1984) studied steady flow over an oscillating flap mounted on a flat plate. Reynolds & Carr (1985) in their recent review offer some ideas about the mechanisms by which vortices form under such conditions. Taneda (1979) used streamline visualization for steady flow over fences, double steps and cavities at very low Reynolds numbers, examples of which are reproduced for easy access by Van Dyke (1982). At higher Reynolds numbers fluctuations occur over cavities, a situation prone to sound generation. We refer to the distinguished work by Rockwell & Knisely (1979).

2. Experimental set-up and methods

Visualization experiments were conducted in a low-speed wind tunnel which was modified according to Freymuth, Bank & Palmer (1983) to generate for 4 s after start from rest a flow of constant acceleration $a = 2.4\ \mathrm{m\ s^{-2}}$. For photographic observation the top and front walls of the tunnel were made from Plexiglas while the floor and back walls were painted black. The experiment was floodlit from the top and photographed from the front space using a 16 mm movie camera at a rate of 64 frames/s. Visualization was by the titanium-tetrachloride method described by Freymuth, Bank & Palmer (1985).

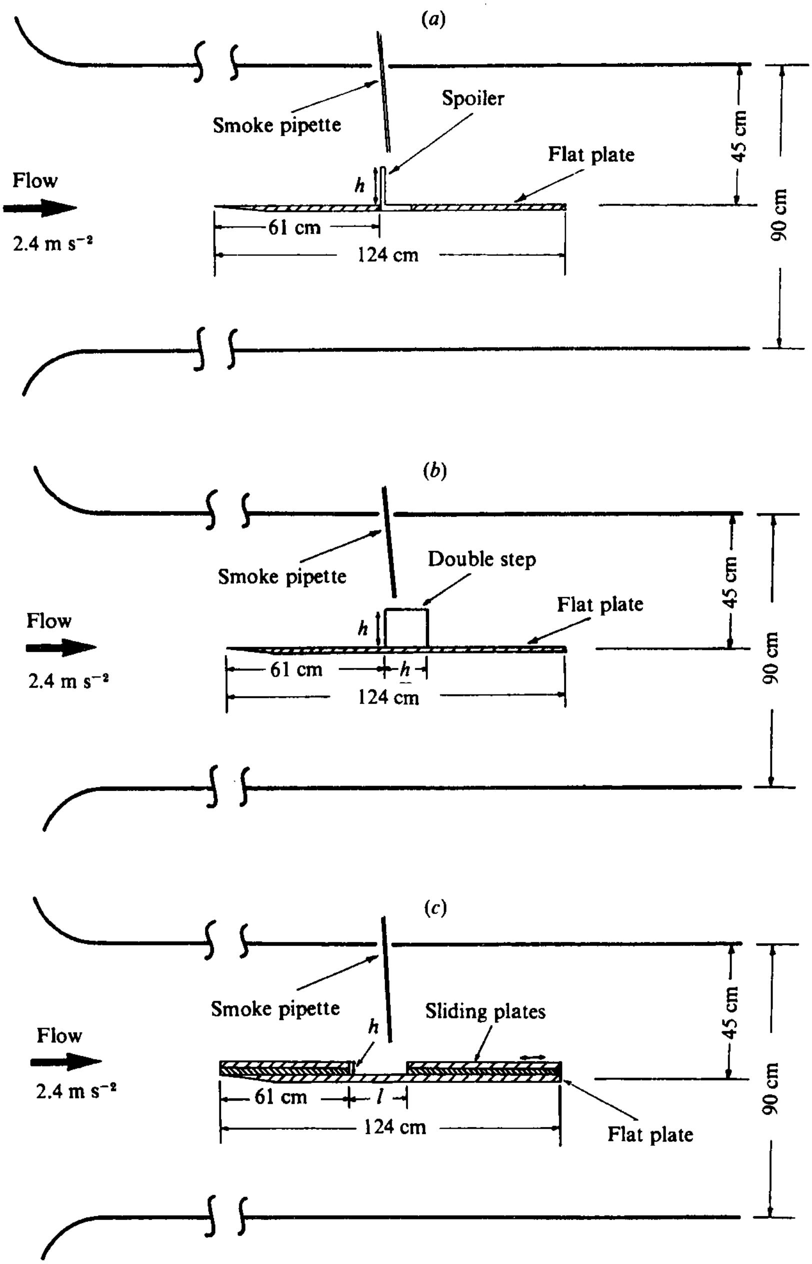

FIGURE 1. Experimental set-up for (*a*) spoiler flow visualizations, (*b*) double-step flow visualizations, and (*c*) cavity flow visualizations.

A flat plate was mounted on the sidewalls of the wind tunnel in the middle of the test section. A spoiler of height h was installed on the plate as sketched in figure 1 (*a*), or a double step was mounted as sketched in figure 1 (*b*). A cavity flow was established by using sliding flat plates of 1.9 cm thickness mounted on top of the original plate as sketched in figure 1 (*c*). The cavity height was varied by using additional plates

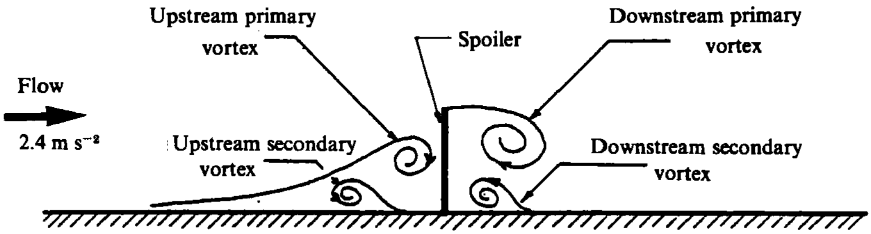

FIGURE 2. Sketch of the two-dimensional vortices that may develop over spoiler in accelerating flow.

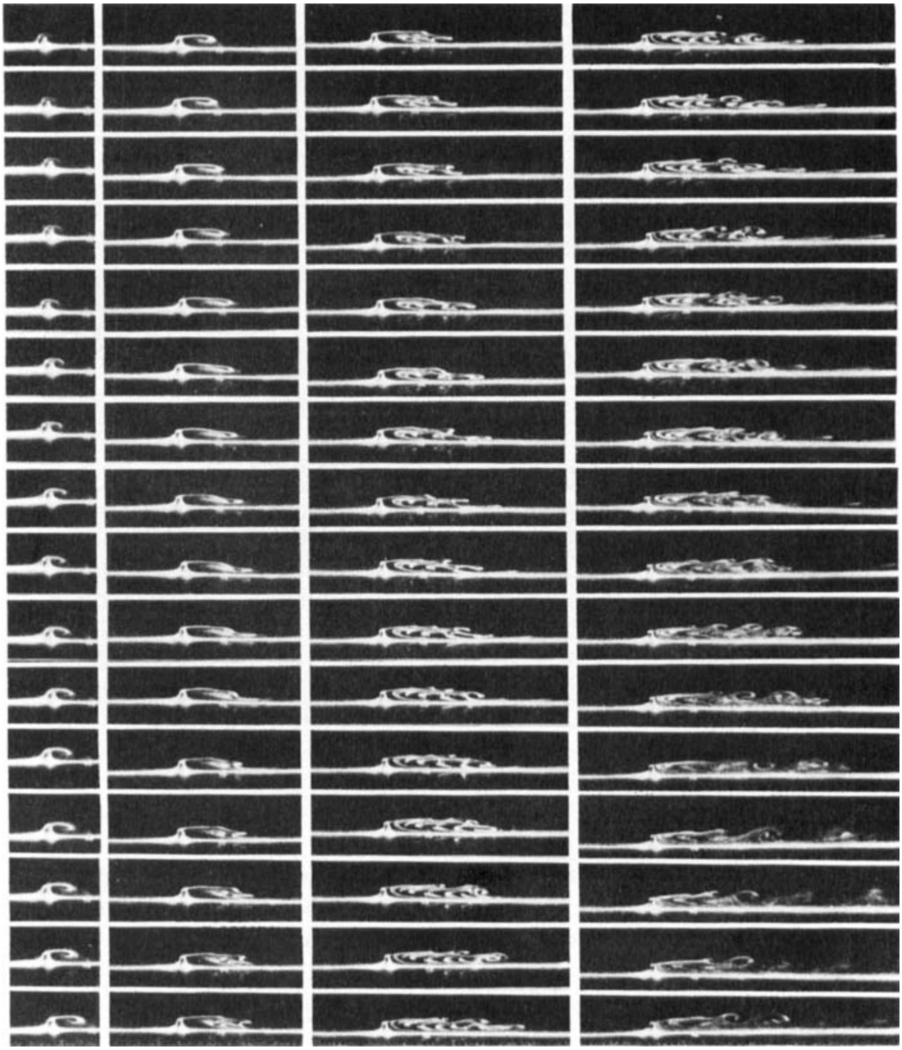

FIGURE 3. Sequence of accelerating-flow development over spoiler. $a = 2.4$ m s^{-2}, $h = 0.64$ cm, $Re = 124$ (defined in equation (1)), $t_1 = \frac{15}{64}$ s, $\Delta t = \frac{1}{64}$ s.

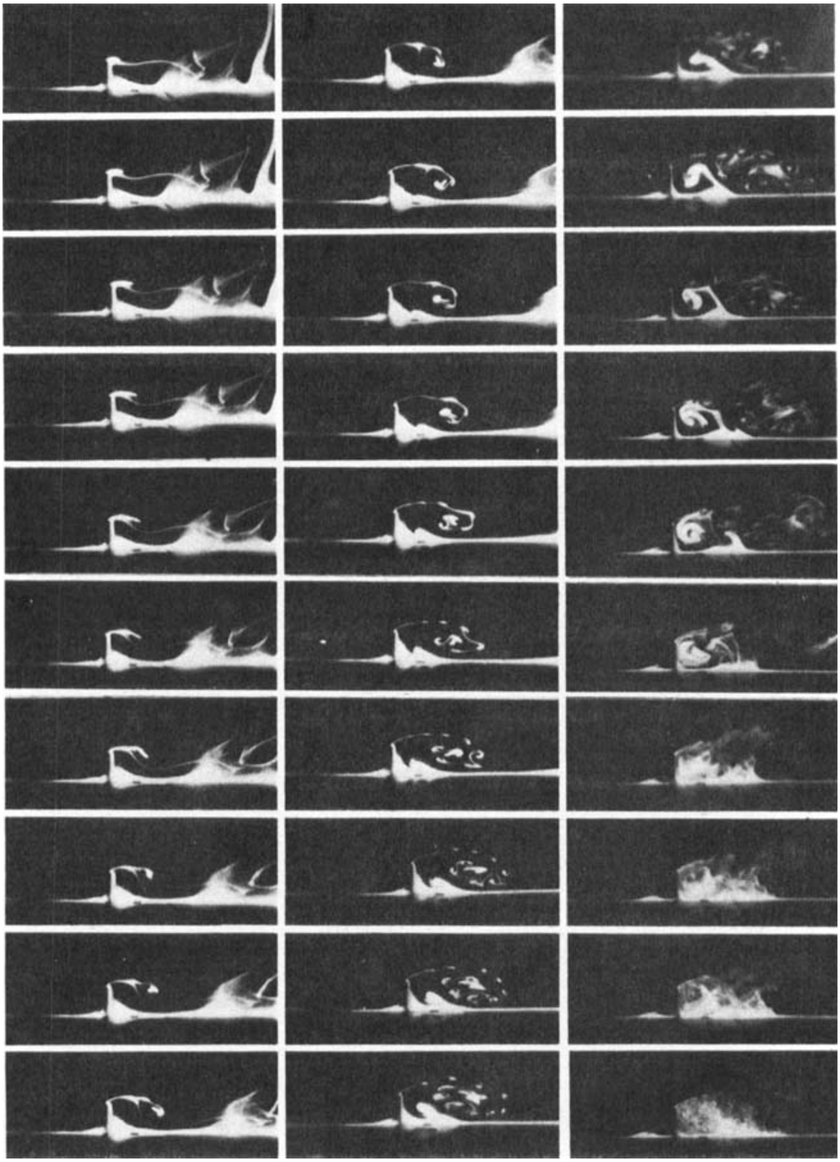

FIGURE 4. Sequence of accelerating-flow development downstream of a spoiler. $a = 2.4\ \mathrm{m\ s^{-2}}$, $h = 2.54$ cm, $Re = 1000$, $t_1 = \frac{11}{64}$ s, $\Delta t = \frac{1}{32}$ s.

of the same thickness. Cavity length was varied by moving the sliding plates either forward or backward. Owing to the blunt front of these plates, a front disturbance reached the cavity after some time but visualization was prior to this time.

3. Results of visualization

In this section we present our photographic sequences of vortex development and accompanying descriptions. Frames of a sequence were ordered into columns from top to bottom with columns ordered from left to right. The time from flow start-up

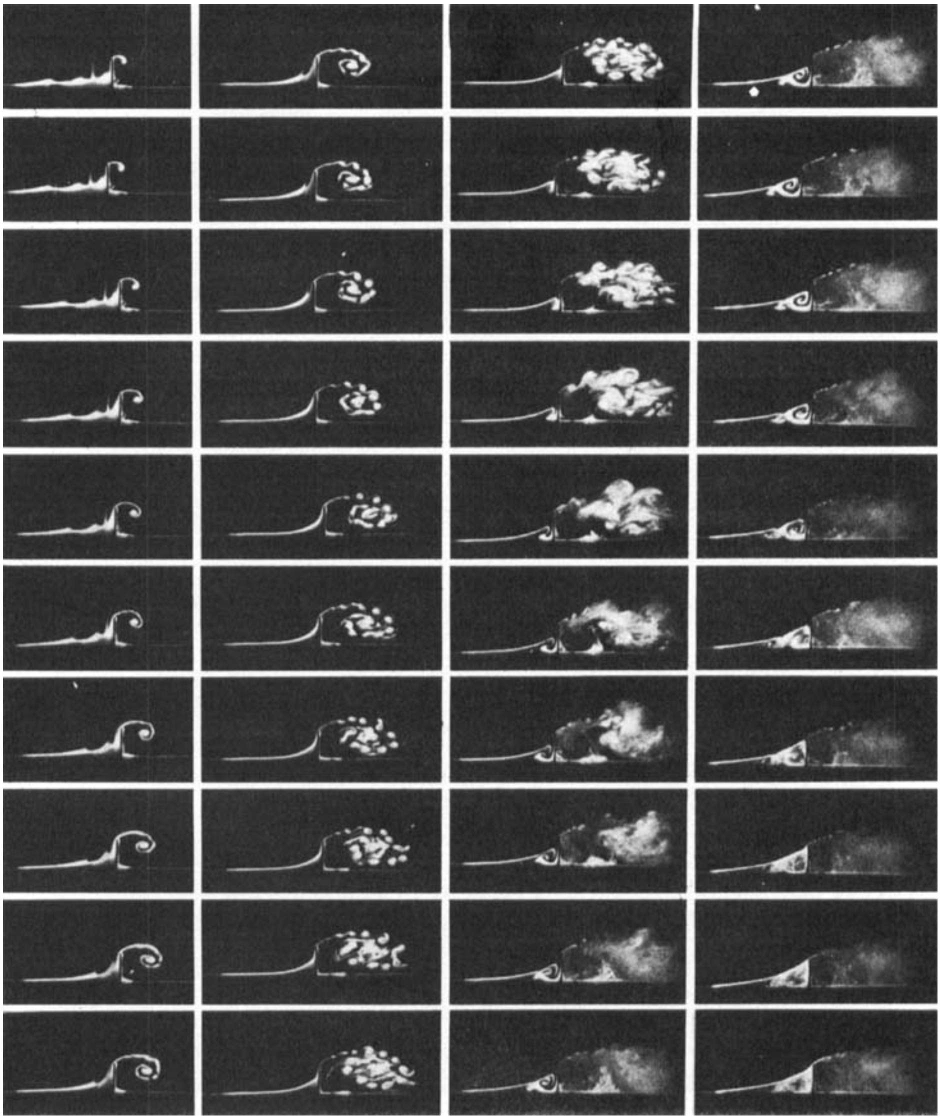

FIGURE 5. Sequence of accelerating-flow development over a spoiler. $a = 2.4\ \mathrm{m\ s^{-2}}$, $h = 5.1$ cm, $Re = 2800$, $t_1 = \frac{22}{64}$ s, $\Delta t = \frac{1}{32}$ s.

to the first frame shown in a sequence is labelled t_1, and the time between consecutive frames is Δt; these times are listed in the figure caption for each sequence. Flow is always from left to right.

3.1. *Accelerating flow over spoilers*

Before presenting photographic sequences let us sketch in figure 2 the vortices which may develop some time after flow start-up. The sketch shows the downstream primary vortex, which quickly separates from the spoiler edge, as well as a downstream secondary vortex which may develop later. In the upstream region separation occurs later and forms a primary and a secondary vortex.

A first sequence of photographs is presented in figure 3, which features some but

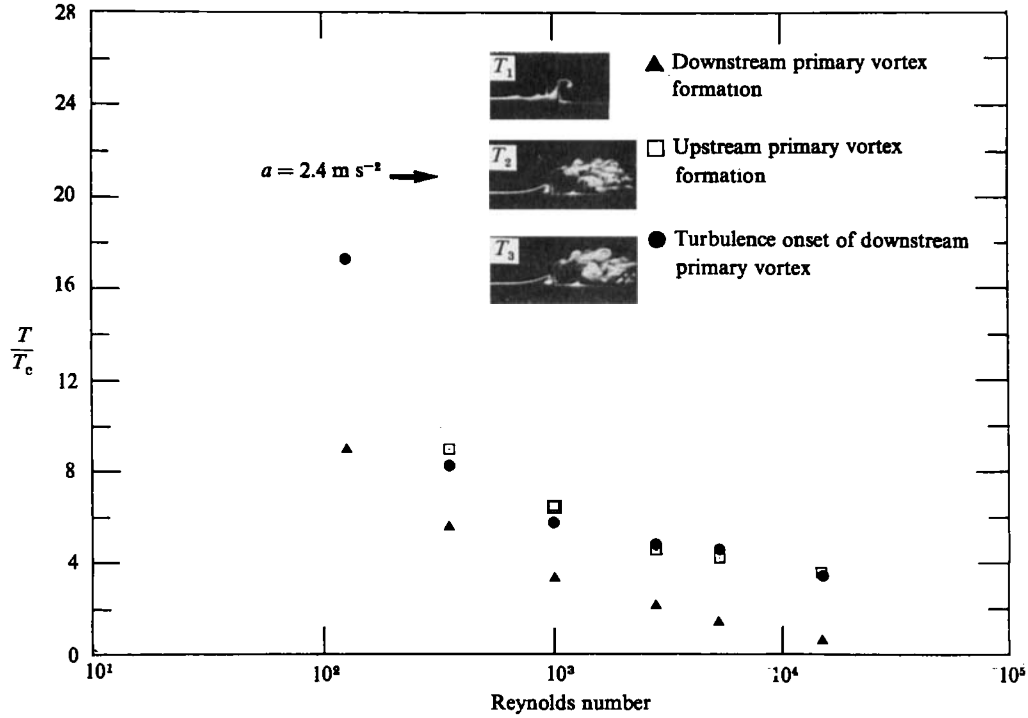

FIGURE 6. Dimensionless times T_1/T_c, T_2/T_c, T_3/T_c for accelerating flow over spoilers, as a function of Reynolds number.

not all of the characteristics sketched in figure 2. This sequence was taken for a small spoiler with height $h = 0.64$ cm which corresponds to a Reynolds number $Re = 124$. The Reynolds number is defined by

$$Re = (2h)^{\frac{3}{2}} a^{\frac{1}{2}} \nu^{-1}, \quad (1)$$

where ν is the kinematic viscosity of air. In column 1 separation of a vortex filament from the top of the spoiler occurs and subsequently a vortex loop forms which establishes the primary downstream vortex. In column 2 some stretching of this vortex loop occurs in the vicinity of the flat plate. In addition some waviness develops in the filament, indicating filamentary instability. In column 3 the vortex pattern becomes highly ornamental and elongated, presumably by filamentary instability and interaction with the flat surface. An intricate pattern like this has not been observed before by us in starting flow over airfoils. In column 4 a new process of vortex pinching close to the flat surface may be recognized, where a vortex loop bears down on vorticity below and ahead of it, in essence pressing this vorticity forward and shaping it into an elongated loop. Several vortices are formed this way and move to the right before the onset of turbulence blurs further detail of pattern development. At this low Reynolds number formation of primary and secondary vortices cannot be identified in the upstream region.

Figure 4 visualizes the vortex development downstream of a spoiler of height $h = 2.54$ cm corresponding to $Re = 1000$. As before separation of a vortex filament, formation of a loop and ornamentation can be observed except that the onset of

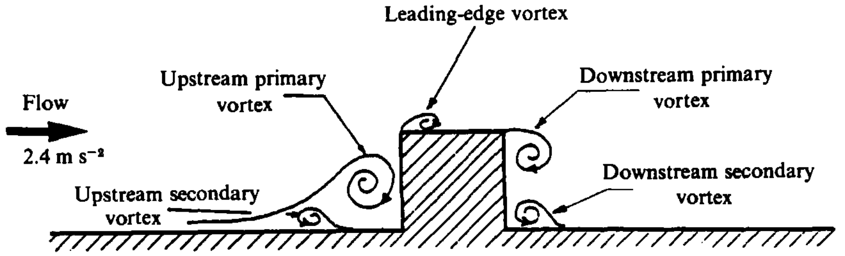

FIGURE 7. Sketch of two-dimensional vortices that may develop over a double step in accelerating flow.

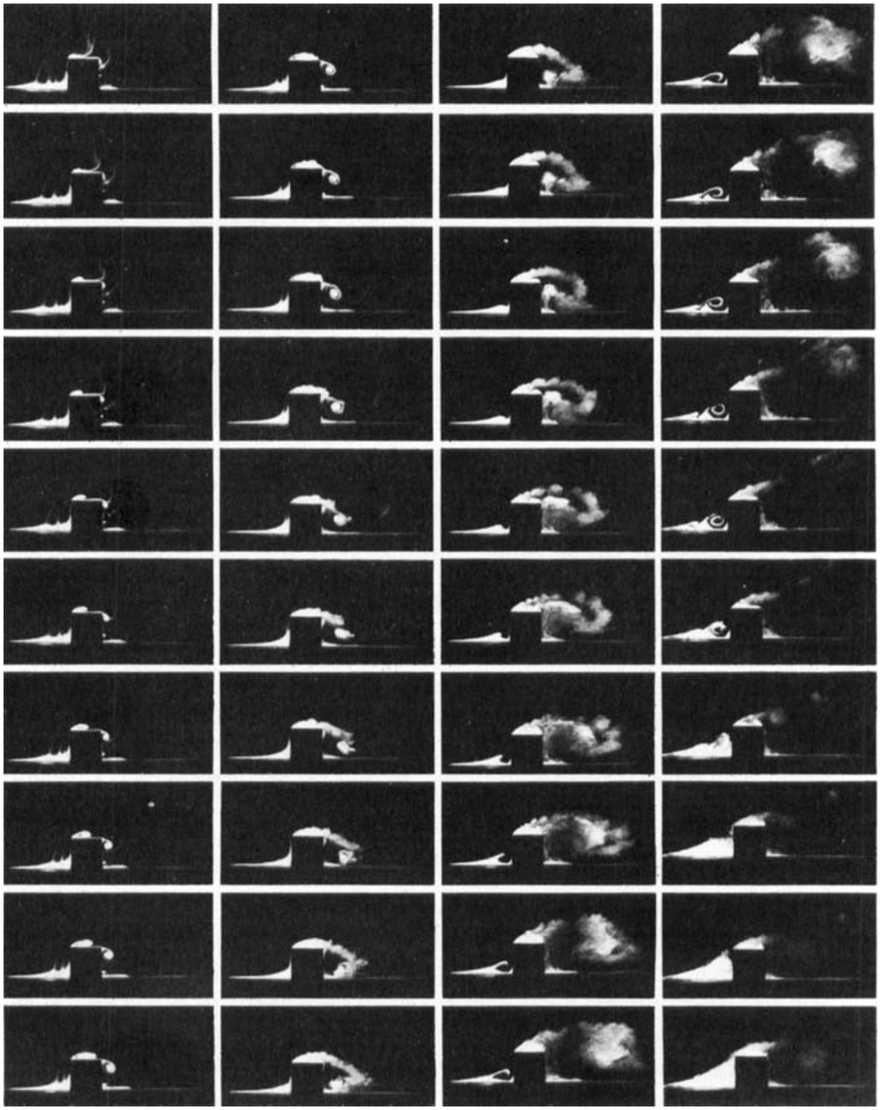

FIGURE 8. Sequence of accelerating-flow development over double step. $a = 2.4 \text{ m s}^{-2}$, $h = 10.16$ cm, $Re = 7800$, $t_1 = \frac{19}{64}$ s, $\Delta t = \frac{1}{32}$ s.

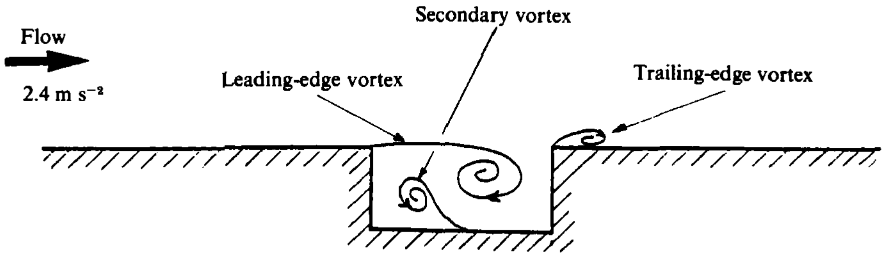

FIGURE 9. Sketch of two-dimensional vortices that may develop over a cavity in accelerating flow.

turbulence in column 3 prevents a highly elongated ornamental structure. At this Reynolds number we can clearly see the formation of a downstream secondary vortex in column 2 and the upper frames of column 3.

Figure 5 visualizes the overall vortex development over a spoiler of height $h = 5.1$ cm, corresponding to $Re = 2800$. Smoke was introduced upstream of the spoiler and on its edge. Formation, ornamentation and onset of turbulence for the primary vortex appear very clear. The secondary vortex is only hinted at in column 3. Column 3 shows in addition the rather late formation of the upstream primary vortex, and the first few frames of column 4 show the subsequent formation of an upstream secondary vortex.

In addition to the sequences documented in figures 3–5 other spoiler heights were introduced to allow an analysis of Reynolds-number dependence of events over time. A similar analysis has been presented for airfoils by Finaish, Palmer & Freymuth (1984), where details of evaluations are given.

Figure 6 shows the dependence of times T_1, T_2 and T_3 on Reynolds number, where T_1 is the time from flow start-up to the formation of the downstream primary vortex, T_2 is the corresponding time for upstream vortex formation and T_3 is the time to the onset of turbulence for the downstream primary vortex. The photographic insets show typical vortex patterns at these times. Times were non-dimensionalized by means of a characteristic time defined by

$$T_c = (2h)^{\frac{1}{2}} a^{-\frac{1}{2}}. \tag{2}$$

From figure 6 the following results are obtained: all three dimensionless times (T_1/T_c, T_2/T_c, T_3/T_c) decrease with increasing Reynolds number. The dimensionless time difference $(T_2 - T_1)/T_c$ is approximately independent of Reynolds number except at $Re = 124$ where turbulence sets in late. Dimensionless times T_2/T_c and T_3/T_c are approximately the same, except that at $Re = 124$ an upstream vortex was not identifiable by us.

3.2. *Accelerating flow over double steps*

Exploring for new unsteady vortex patterns we considered the vortical development over a square double step which may be considered to be a generalized spoiler with a substantial spoiler width l compared to its height h. Figure 7 sketches possible vortical developments which may occur, i.e. the addition of a leading-edge vortex which does not exist for the usual spoiler.

These concepts can be observed in the sequence presented in figure 8. Photographs in column 1 show formation of the leading-edge and downstream primary vortex. Turbulence starts in column 2 where it first affects the leading-edge vortex, then the downstream vortex. In column 3 these vortices have merged into one. The upstream

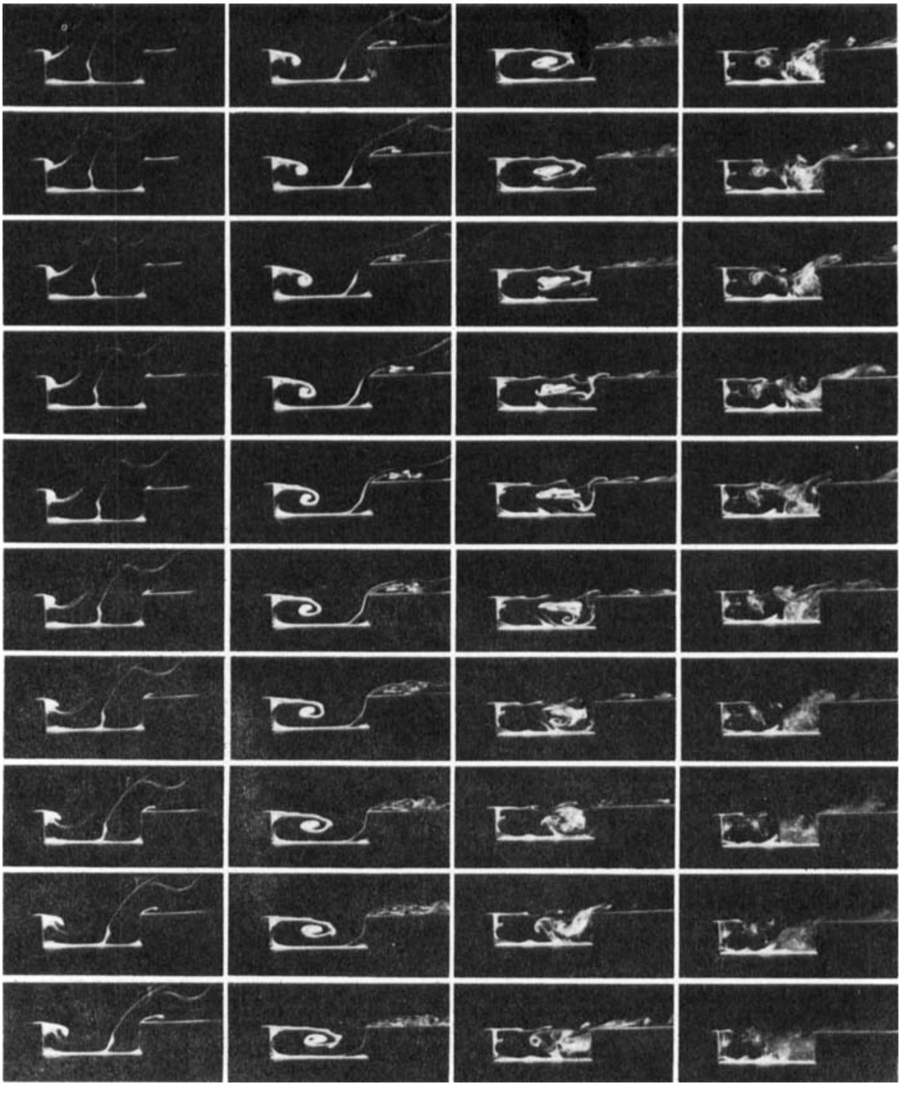

FIGURE 10. Sequence of accelerating-flow development over a cavity. $a = 2.4\ \mathrm{m\ s^{-2}}$, $h = 3.81$ cm, $l = 12.7$ cm $Re = 1800$, $t_1 = \frac{14}{64}$ s, $\Delta t = \frac{1}{32}$ s.

primary vortex forms in the lower part of column 3 and the associated secondary vortex forms in the upper part of column 4. Turbulence starts for the upstream patterns in the lower part of column 4. The downstream secondary vortex is not well visualized in this sequence.

3.3. *Accelerating flow over cavities*

Figure 9 sketches the main vortices whose formation may be anticipated in cavity flow, i.e. leading- and trailing-edge vortices and a secondary vortex inside the cavity.

As an example, figure 10 visualizes accelerating flow over a cavity with the relevant conditions given in the figure caption. Column 1 shows leading- and trailing-edge separation. Column 2 reveals the growth and ornamentation of the leading-edge vortex and the onset of turbulence for the trailing-edge vortex. In column 3 the leading-edge vortex moves toward the trailing edge and impinges on it in frame 4, where an interesting triarm pattern exists. Impingement causes some of the vorticity to move over the cavity and some into the cavity, by the same process which for steady outer flow has been termed vortex severing by Rockwell & Kniseley (1979). Development of a secondary vortex inside the cavity can barely be seen in the lower half of column 3 before turbulence blurs any further detail of pattern development. The accelerating flow was visualized for a range of l/h between 0.33 and 8. For deep cavities ($l/h < 2$), the leading-edge vortex inside the cavity rotates without any interaction with the cavity trailing edge, and no secondary vortex develops inside the cavity.

4. Concluding remarks

New patterns of two-dimensional vortices in starting flows of highly angular geometries have been documented and described with only minor attention given to parametric detail. These patterns should add to the wealth of dynamic vortices which have been documented in the past and should serve as references for future numerical experiments.

The authors would like to thank Mr R. Meinzer for his technical assistance. This work was supported by the AFOSR grant number 81-0037.

REFERENCES

FINAISH, F., PALMER, M. & FREYMUTH, P. 1984 A parametric analysis of vortex patterns visualized behind airfoils in accelerating flow. *Ninth Symp. on Turbulence, 1–3 Oct., 1984, Rolla, Missouri, preprint vol., paper no.* 10, p. 10–1.

FRANCIS, M. S., KEESE, J. E., LANG, J. D., SPARKS, G. W. & SISSON, G. E. 1979 Aerodynamic characteristics of an unsteady separated flow. *AIAA Paper* 17-1332.

FREYMUTH, P. 1985 The vortex patterns of dynamic separation: a parametric and comparative study. *Prog. Aerospace Sci.* **22**, 161.

FREYMUTH, P., BANK, W. & PALMER, M. 1983 Visualization of accelerating flow around an airfoil at high angles of attack. *Z. Flugwiss. Weltraunforschung* **7**, 392.

FREYMUTH, P., BANK, W. & PALMER, M. 1985 Use of titanium tetrachloride for visualization of accelerating flow around airfoils. *Flow Visualization* III, Hemisphere 99.

KOGA, D. J., REISENTHEL, P. & NAGIB, H. M. 1984 Control of separated flow fields using forced unsteadiness. *IIT Heat Transfer and Fluids Rep.* R-84-1. Illinois Institute of Technology.

REYNOLDS, W. C. & CARR, L. W. 1985 Review of unsteady, driven, separated flows. *AIAA paper* 85-0531.

ROCKWELL, D. & KNISELY, C. 1979 The organized nature of flow impingement upon a corner. *J. Fluid Mech.* **93**, 413.

TANEDA, S. 1979 Visualization of separating Stokes flows. *J. Phys. Soc. Japan* **46**, 1935.

VAN DYKE, M. 1982 *An Album of Fluid Motion*. Parabolic.